Journal of Materials Chemistry C

Accepted Manuscript

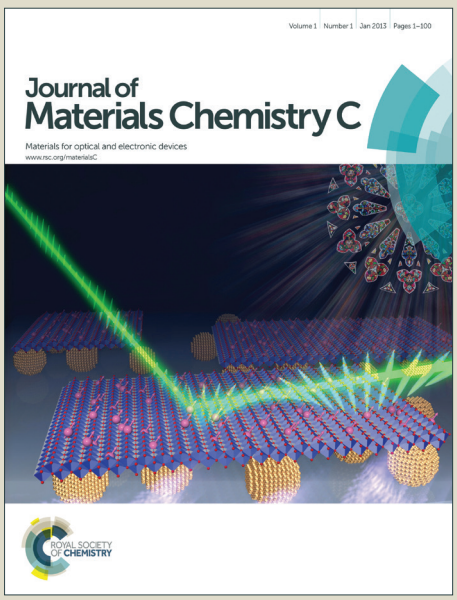

ROYAL SOCIETY OF CHEMISTRY

www.rsc.org/materialsC

Journal of Materials Chemistry C

Dynamic Article Links►

Cite this: DOI: 10.1039/c0xx00000x

PAPER

www.rsc.org/xxxxxx

Highly efficient warm white light emitting Eu^{2+} activated silicate host: Another fabulous work of mesoporous silica

Sakthivel Gandhi,[a,b] Kavitha Thandavan,[b] Bong-Joon Kwon,[a] Hyun-Joo Woo,[a]Chang Hae Kim,[c] SoungSoo Yi,[d] Jung Hyun Jeong,[e] Dong-SooShin[f] and Kiwan Jang*[a]

Received (in XXX, XXX) XthXXXXXXXXX 20XX, Accepted Xth XXXXXXXXX 20XX

DOI: 10.1039/b000000x

This piece of work outlines a novel approach towards the synthesis of an efficient yellow emitting $Sr_{0.975}Ca_{0.975}Eu_{0.05}SiO_4$ phosphor imbibed with the sufficient red spectral components. This teleportation was achieved by the fidelity of the well-known silicate source namely, mesoporous silica. The findings showed a broad emission of the synthesized phosphor, from blue to red along with a stable emission color till 450 K and emission decay time of 1 µs. When the phosphor is fabricated with ultra-violet (400 nm) and blue LED (450 nm) chips, it promisingly harnessed warm-white light with correlated color temperature < 4000 K, and color rendering index > 80.

Introduction

One among the promising field of research in the development of current generation illumination device is the Light Emitting Diodes (LED).[1] White light emitting diodes offer considerable advantage over the conventional lighting sources namely incandescent, fluorescent lamps and high intensity discharge lamps in terms of longer life time, efficiency, power consumption, compactness and rigidity, eco-friendliness etc.,[1–4] The exploration for a higher-efficiency lighting products is ever increasing and thus LED adds to its momentum. One way to meet out the expectation is by the use of phosphors. Adopting a suitable technology to bring out the potential of the single phosphor converted white light emitting diodes is vital. But an insurmountable barrier rests with the maintenance of circadian rhythm, for it to be utilized for indoor application. In fact, phosphors are the cue for efficiency of LED over other technologies and even among the LED lighting products. With the advent of new phosphors the quality of LED's are being improvised day by day. There are many factors which determine the efficiency of LED phosphors namely the broad emission consisting of more red spectral component from a single phase, good color coordination, CCT (color correlation temperature) <4000 K, CRI (color rendering index) >80, greater thermal stability of material and its emission behavior.[3]

An important challenge in forefront for improving the quality of warm white light LEDs, is the confinement to the particular region of color by a phosphor material. A number of materials had been attempted for the development of high efficiency LED phosphors.[5] Commercial LEDs makes use of YAG:Ce, due to its associated advantages such as the strong absorption in the blue region, emission in broad range from 500-700 nm, high quantum efficiency and fast luminescence decay time.[6]Despite the necessary technical improvements, it fails in satisfying the red spectral component which results in its limitations namely high CCT and low CRI. All these factors will lead to a bluish-cold illumination which is unsuitable for the indoor illumination. These deficits were tried to overcome by following two different strategies among which, one is the multi emitting centers conversion and the other is multi phosphor conversion models. The former one is based on the introduction of some red emitting dopants to the single yellow (or green) emitting phosphor (for an instance YAG:Ce)[6] while the latter one derives the additive effect of different color emitting phosphors to harvest warm white light.[7] But, the exploration for the perfect phosphor still goes on and the best fit is expected in terms of a highly efficient single phosphor converting warm white light which covers a broad area of emission along with a suffice red spectral component (CCT<4000 K & CRI>80). Here we have chosen a divalent Eu doped $SrCaSiO_4$as host and achieved the longer wavelength broad emission along with the required red spectral components by the virtue of mesoporous silica (MPS) as silicate source through a simple wet-solid phase reaction method.

A comprehensive probe into the literature reveals a wide variety of silicate-based phosphors.[8,9] Their successful synthesis was achieved only because of the suitable method adopted. The best method should pave the way for the uniform distribution of the Eu^{2+}activators and it is possible only in the case of solution based techniques rather than the conventional solid state reactions. The main water dispersible silica source used so far is SiO_2[8–10] and propylene glycol-modified silane (PGMS).[11] Previously, our group reported a $CaSrSiO_4$ phosphor using organic tetraethyl orthosilicate (TEOS) as the silica source.[12]

Though it was an excellent contestant in this competition it fails in many of the aspects. A close observation into it helped us to alleviate this deficit (i.e.,) alteration of the silica source changes the occupancy of dopant in cationic site of crystal by which the efficiency can be fine-tuned rather than its retarding effect.

One such material of interest is the mesoporous silica, which can very well be ascribed as the material of the century. Mesoporous silica is a well-known versatile material owing to its inherited advantages namely the chemical and thermal stability, excellent charge transfer ability, high surface area and its easy tunability.[13]

In our contemporary work, we report the synthesis of $Sr_{0.975}Ca_{0.975}Eu_{0.05}SiO_4$ phosphor using the simple wet-solid phase reaction method. The key to innovation in this reaction is the use of mesoporous silica (MPS) as the silicate source. The results showed a broad yellow emission with a broad regimen from blue to red along with the requisite red spectral component. Thus a novel silica source was attempted with success and thus an efficient phosphor for making warm-white light was obtained along with CCT < 4000 K & CRI > 80.

Results & Discussion

The phase purity of the as-synthesized ($Sr_{0.975}Ca_{0.975}Eu_{0.05}^{(3+)}SiO_4$) and final MPS assisted $Sr_{0.975}Ca_{0.975}Eu_{0.05}SiO_4$ phosphors were analyzed using x-ray powder diffraction and are shown in Figure 1. The X–ray diffraction patterns are in good agreement with the standard card ICSD no. 049660 and JCPDS no. 01-077-1619.[10] Additionally, specific structural analysis has been reported for the same composition, elsewhere[10] and it is overlaid in the aforementioned figure (Figure 1). To be more precise, the XRD pattern observed for both the as-synthesized and final MPS assisted $Sr_{0.975}Ca_{0.975}Eu_{0.05}SiO_4$ samples confirmed the orthorhombic α′$SrCaSiO_4$ phase with a *Pmnb* space group. The lattice parameters are found to be as a = 5.6049 Å; b = 6.9623 Å; c = 9.463 Å & V = 370.05 $Å^3$. It was also observed that the inception of Eu^{2+} to the crystal lattice does not cause any significant impact to the crystal structure. This confirms that the introduction of Eu ions doesn't create a new crystal phase instead; it gently replaces the cationic sites of Ca^{2+} and Sr^{2+} ions of the orthorhombic crystal lattice. A notable increase in crystallinity was observed when the sintering temperature is greater than1200 °C. But, the optimum sintering temperature was fixed to be 1200 °C based on its luminescence efficiency. Several reports are detailing with the synthesis of similar crystals doped with divalent Eu ions and by the usage of various silicate sources ranging from conventional silica to organic silica sources are available.[8–12] Tezuka*et al.* reported the synthesis of $SrCaSiO_4$:Eu^{2+} phosphor using novel water soluble silica as silicate source.[11] Our work is the first of its kind towards the synthesis of phosphor or a crystal lattice using amorphous mesoporous silica as silicate source.

The amorphous nature of MPS was confirmed from the X-ray diffraction pattern which is shown in Figure S1(a). The intrinsic features of MPS are quite obvious from SEM (Figure 2), TEM (Figure S1-b) & nitrogen physisorption isotherm studies (Figure S1-c&d). These studies confirm the high surface area (750 m^2/g), ordered porous structure along with the size and volume of 7 nm & 1.12 cm^3/g, respectively. A comparative study of the conventional silica and MPS reveals the difference in their physical properties which are tabulated and shown in the supplementary material (Table S1). Thus the distinct features of MPS over conventional silica sources are clearly discernible. The FE-SEM observations of MPS, as-synthesized and final MPS assisted $Sr_{0.975}Ca_{0.975}Eu_{0.05}SiO_4$phosphorsare shown in Figure 2. The images clearly exhibits the regular and partially regular particles of as-synthesized (Figure 2c) and final MPS assisted $Sr_{0.975}Ca_{0.975}Eu_{0.05}SiO_4$ phosphors (Figure 2d), respectively. Moreover, it mimics the morphology of MPS with the sizes around 1 μm (Figure 2a). An irregular morphology is observed in the case of final MPS assisted $Sr_{0.975}Ca_{0.975}Eu_{0.05}SiO_4$ phosphor and this can be attributed to the applied high sintering temperature which leads to fusion. The EDS spectrum of the synthesized phosphor revealed peaks of Ca, Sr, Si, Eu and O (Figure S2) and was quantitatively measured to be ~ 19, 25, 35 & 0.47% for Sr, Ca, Si & Eu, respectively.

The excitation emission behaviour of the MPS assisted $Sr_{1-x}Ca_{1-x}Eu_{2x}SiO_4$ phosphor was envisaged using a spectrofluorimeter. Primarily, the concentration dependant luminescence spectra were recorded at 375 nm of emission wavelength for MPS assisted $Sr_{1-x}Ca_{1-x}Eu_{2x}SiO_4$ (2x = 0.0025, 0.005, 0.01, 0.05, 0.075 and 0.1) phosphors (Figure S3) for the determination of optimum dopant concentration. All the samples showed a similar trend with a very broad emission band from 450 nm to 700 nm with a peak centered at ~585 nm. A proportional increase in emission intensity is observed with the dopant concentration till 0.05 and further increase in concentration leads to decremented value. This may be ascribed to the occurrence of non-radiational transition between Eu ions that leads to the concentration-quenching and thus reducing the intensity of emission. Hence, the optimum concentration was fixed to be 0.05 and $Sr_{0.975}Ca_{0.975}Eu_{0.05}SiO_4$ had been taken for further analysis. Figure 3 shows the normalized excitation and emission spectra of MPS assisted $Sr_{0.975}Ca_{0.975}Eu_{0.05}SiO_4$phosphor recorded at room temperature. The excitation spectrum of the sample monitored at 585 nm emission covers the near ultra violet (NUV) and blue regions (from 300 to 500 nm), and it showed the presence of two bands with the peak centered at ~375 and ~420 nm ($4f^7 \rightarrow 4f^6 5d^1$). This can be very well assigned to the occupancy of Eu^{2+} at two different sites in the host. The emission spectrum recorded at 375 nm of excitation was also shown in the same Figure. It showed a very broad Eu^{2+} emission band (450–700 nm) that centered at ~585 nm and covers a wide spectral region ranging from blue to red. The emission band of MPS assisted $Sr_{0.975}Ca_{0.975}Eu_{0.05}SiO_4$ phosphor exhibits full width half maxima (FWHM) of ~150 nm which is greater than the FWHM of conventional YAG:Ce and SiO_2 assisted $SrCaSiO_4$:Eu^{2+}(Table S2).

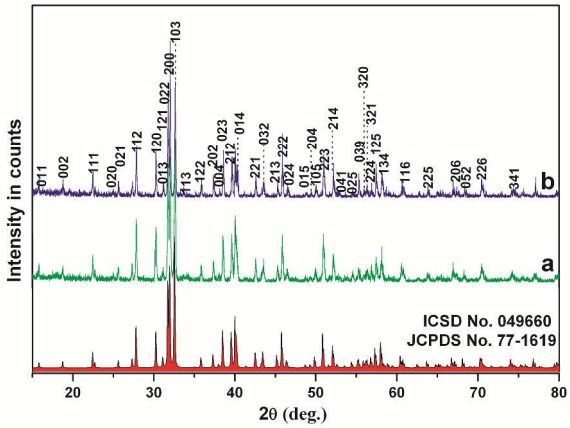

Figure 1. Powder X-ray diffraction patterns of as-synthesized (a) and final (b) MPS assisted $Sr_{0.975}Ca_{0.975}Eu_{0.05}SiO_4$ phosphor, indexed to the orthorhombic $SrCaSiO_4$ from ICSD (049660) and JCPDS (77-1619) data base.

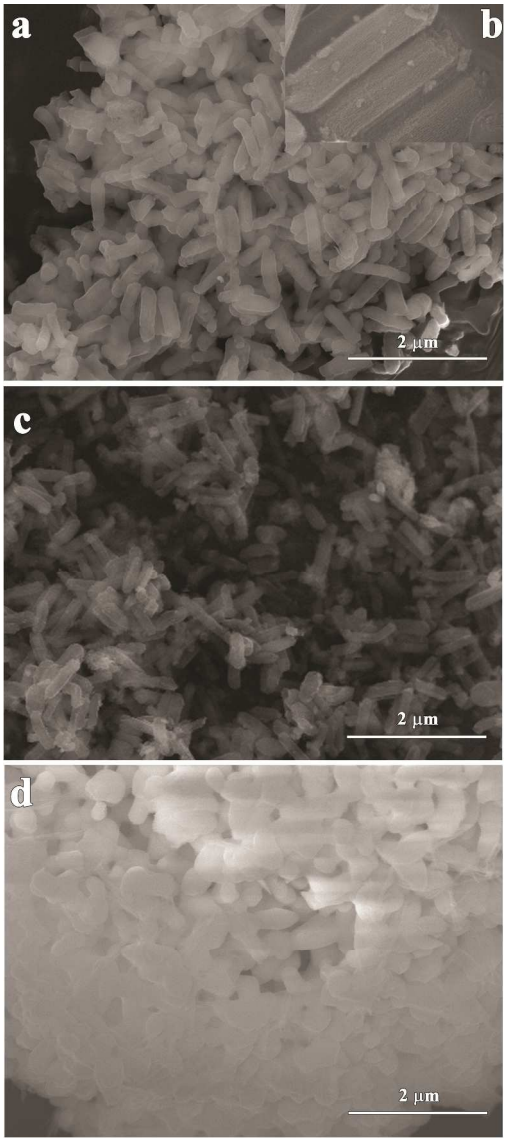

Figure 2. FE-SEM images of low (a) & high magnified MPS (b), as-synthesized(c) and final MPS assisted $Sr_{0.975}Ca_{0.975}Eu_{0.05}SiO_4$ phosphor (d).

The relative study on emission behavior of various samples namely MPS assisted $Sr_{0.975}Ca_{0.975}Eu_{0.05}SiO_4$ (recorded at 375 nm excitation), conventional SiO_2 assisted $SrCaSiO_4$ (recorded at 370 nm excitation) and commercial YAG:Ce (recorded at 440 nm excitation) are shown in Figure S4. This shows the improvised features of the MPS material in the synthesis of silicate phosphors in terms of threefold increase in the intensity to the phosphor synthesized using conventional SiO_2 (Figure S4-a). The FWHM of conventional SiO_2 assisted $SrCaSiO_4$ and commercial YAG:Ce is 100 & 70 nm, respectively. The FWHM value of the MPS assisted $Sr_{0.975}Ca_{0.975}Eu_{0.05}SiO_4$ phosphor is relatively much greater than that of the normal Eu^{2+} introduced phosphors and commercial YAG:Ce phosphors as well. This indicates that the broad band yellow emission observed in MPS assisted $Sr_{0.975}Ca_{0.975}Eu_{0.05}SiO_4$ is the unique feature associated with it than that of the normal Eu^{2+} $4f^65d^1 \rightarrow 4f^7$ emission.

A further detailed study was carried out to understand the energy transfer and emission mechanism of Eu^{2+} in the MPS assisted $Sr_{0.975}Ca_{0.975}Eu_{0.05}SiO_4$ host, where the band is split using Gaussian method (Figure S5). The Gaussian fit shows the clear splitting of two bands which are located at 510 nm and 585 nm. The existence of two bands may be attributed to the locus of dopant in two different cationic sites (C1 & C2) whose co-ordination numbers are 8 and 10, respectively. For instance, the prior one in C1 shows the shorter wavelength and the latter one at C2 shows the emission at longer wavelength. As shown in Table 1, the ionic radii of Eu^{2+} at both the co-ordination numbers are almost equal or lesser than that of the ionic radii of Sr^{2+}, but in the case of ionic radii of Ca^{2+}, it is lesser than that of Eu^{2+}. When the Eu^{2+} is introduced as dopant to the host crystal lattice, if it occupies the cationic site which is smaller than its radii (Ca^{2+} site) for instance, there will be emission at shorter wavelength (510 nm) and this may be ascribed to the increase in crystal field strength. On the other hand, if Eu^{2+} occupies the more favourable Sr^{2+} site, as its radii is either equal to or larger in size than Eu^{2+}, results in the emission at longer wavelength (585 nm). Thus, the high intense emission at longer wavelength can be attributed to the occupation of more favourable Sr^{2+} site by Eu^{2+}, while the occupation of less favourable Ca^{2+} site gives rise to less intense shorter wavelength emission. The difference in the emission mechanism may be ascribed to the formation of linear chain lattice by the cations in addition to the parameters namely covalency, size of the cation and crystal field strength.[9] In the case of MPS assisted $Sr_{0.975}Ca_{0.975}Eu_{0.05}SiO_4$ host lattice, the emission was observed at longer wavelength along with a greater Stokes Shift (~9570 cm^{-1}) and FWHM (~4690 cm^{-1}). This increased Stokes Shift may be due to the more delocalization of preferentially oriented d-orbital and this can be attributed to the linear chain lattice formation. In addition to the presence of anionic neighbours, the occurrence of cationic neighbours in the direction of linear chain lattice, the positive charges are experienced by the divalent europium ion. These positive charges are responsible for the preferential orientation of the d-orbital in the linear chain lattice which results in lowering energy and therefore shifts the emission to longer wavelength. Thus, the formation of linear chain lattice with high co-ordination number, promotes the longer emission wavelength and this can be very well assigned to the inception of high surface area MPS whose

morphology and porous structure are highly ordered (Figure S1).

Table 1. Ionic radius of Ca^{2+}, Sr^{2+} and Eu^{2+}.

Co-ordination number	Rare earth and alkali metal ions [14]		
	Eu^{2+} (Å)	Ca^{2+} (Å)	Sr^{2+} (Å)
10	1.35	1.23	1.36
8	1.25	1.12	1.26

The luminescence behaviour of MPS assisted $Sr_{0.975}Ca_{0.975}Eu_{0.05}SiO_4$ phosphor, was measured as the temperature-controlled emission intensities from 273–523 K, and given in Figure 3B. An inverse relation was observed with the factors namely temperature and emission intensity. In the same lines, at the temperature of 450 K, a drop in the emission intensity was observed (i.e.) ~60 % of their values when compared to the temperature of 273 K. This indicates that the quenching temperature for emission intensity is greater than 450 K, which is the characteristic feature of the normal Eu^{2+} $4f^65d^1 \rightarrow 4f^7$ emission. The quenching temperature can be defined as the particular temperature where the intensity is reduced to half of the total value. Likewise, the temperature dependent emission intensity study in the cooling process was carried out from 523 to 273 K (represented by green triangles Figure 3B) and it yielded similar results as that of the heating process. This confirms the recovery of the thermal quenching without causing thermal degradation to our phosphor. Although the emission intensity is temperature dependent, the shape of the emission band of MPS assisted $Sr_{0.975}Ca_{0.975}Eu_{0.05}SiO_4$ remains unchanged from 273 to 523 K (inset of Figure 3B), confirming an excellent and stable color emission of the phosphor.

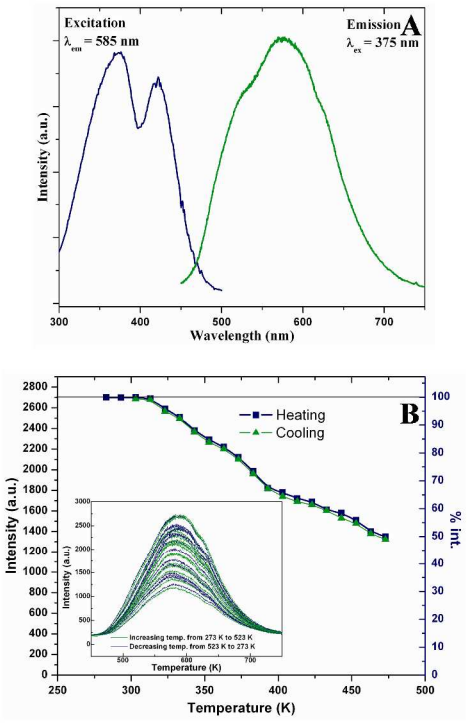

Figure 3. Luminescence properties of MPS assisted $Sr_{0.975}Ca_{0.975}Eu_{0.05}SiO_4$ phosphor (A) Normalized excitation and emission spectra of MPS assisted $Sr_{0.975}Ca_{0.975}Eu_{0.05}SiO_4$ phosphor at room temperature. (B) Temperature dependent emission intensity of MPS assisted $Sr_{0.975}Ca_{0.975}Eu_{0.05}SiO_4$ phosphor excited with 385 nm light at temperature ranging from 273 to 523 K, inset shows the emission spectra recorded during heating (green) and cooling (blue)process as well.

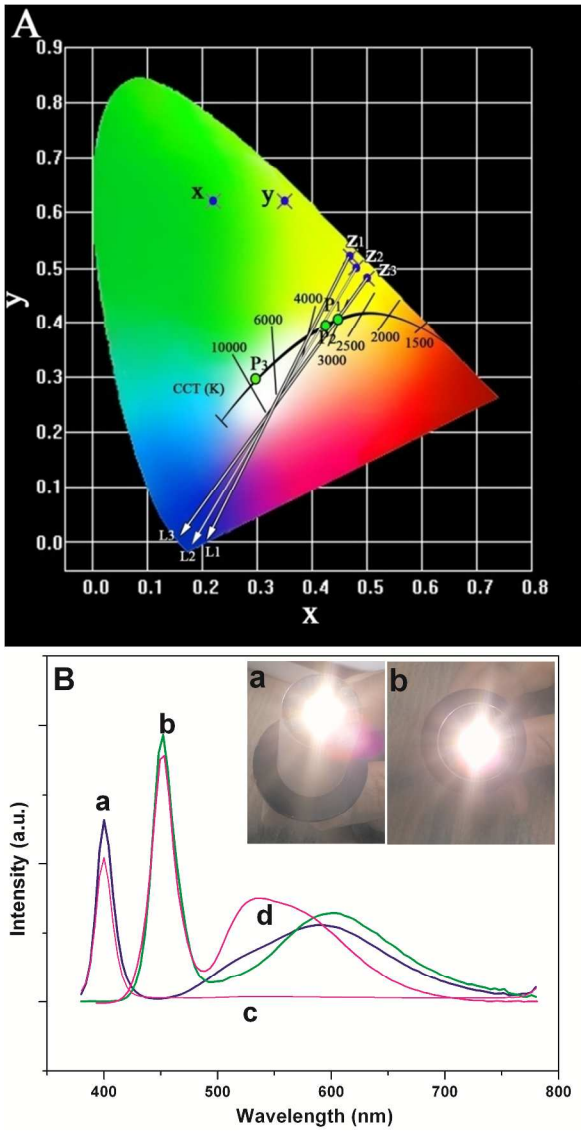

Figure 4. CIE color coordinates and prototype warm-white LEDs.(A) Chromaticity coordinates on CIE 1931 diagram. 'x, y & z' represent the color point of the emission from conventional SiO_2 assisted $CaSrSiO_4:Eu^{2+}$, commercial YAG:Ce& MPS assisted $Sr_{0.975}Ca_{0.975}Eu_{0.05}SiO_4$, respectively. 'L1(380 nm), L2 (400nm) & L3 (450)' are the color point of commercial ultra violet and blue LEDs. The green dots represent the color points of the emission from prototype LEDs fabricated with MPS assisted $Sr_{0.975}Ca_{0.975}Eu_{0.05}SiO_4$ phosphor (P1 with 450 nm & P2 with 400 nm) and commercial YAG:Ce (P3 with 450 nm). The black solid curve is the Planckian locus and the black straight lines are the lines of constant correlated color temperatures from 1500 to 10000 K. (B) Prototype LED emission constructed by embedding the MPS assisted $Sr_{0.975}Ca_{0.975}Eu_{0.05}SiO_4$ phosphor (a & b) and commercial YAG:Ce (c & d) on 400 nm (a & c) and 450 nm (b& d) commercial UV and blue LEDs. Inset is the digital image of designed prototype 400 nm (a) and 450 nm (b) LEDs with our MPS assisted $Sr_{0.975}Ca_{0.975}Eu_{0.05}SiO_4$ phosphor.

All these results show that the yellow emitting MPS assisted $Sr_{0.975}Ca_{0.975}Eu_{0.05}SiO_4$ phosphor possess a very broad band and a single Eu^{2+}emission along with the sufficient red spectral component under near ultra violet and blue light excitations. It also exhibits a good thermal stability along with the stable color emission. All these properties, and precisely the enhancement in red emission, compared with YAG:Ce (Figure S4), make MPS assisted $Sr_{0.975}Ca_{0.975}Eu_{0.05}SiO_4$ a very promising material for achieving warm-white LEDs by a single dopant activated crystal host. Indeed, in their CIE 1931 chromaticity diagram shown in Figure 4A, the intersection of the color point of MPS assisted $Sr_{0.975}Ca_{0.975}Eu_{0.05}SiO_4$ phosphor (z1, z2 & z3)with each of the color point of three commercial near ultraviolet and blue LEDs emitting at 380 (L1), 400 (L2) & 450 nm (L3) are clearly observed (Figure S6). The combination of color coordinates by MPS assisted $Sr_{0.975}Ca_{0.975}Eu_{0.05}SiO_4$ phosphor excited by 380 nm, 400 nm and 450 nm with its corresponding color coordinates of LEDs, results in a warm white light which is marked as a white arrow in the CIE diagram (Figure 4A). On the other hand, the color coordinates of conventional SiO_2 assisted $SrCaSiO_4:Eu^{2+}$showedgreen (x), while the commercial YAG:Ce showed a greenish yellow (y) which results in the production of cold white light with the combination of 450 nm blue LED (P3) due to the lack of required red spectral components. The external quantum efficiency of MPS assisted $Sr_{0.975}Ca_{0.975}Eu_{0.05}SiO_4$ phosphor is calculated to be 72%. This value is higher than that of the conventional SiO_2 assisted $CaSrSiO_4:Eu^{2+}$ and soluble silica assisted $Ca_{0.95}Sr_{0.95}Eu_{0.10}SiO_4$ which showed 45% and 56%,[11,12] respectively. Moreover, the concentration of the dopant used is also very less when compared to the so far reported works in obtaining a yellow or orange $SrCaSiO_4:Eu^{2+}$ phosphor.[8,9,11,12,15]

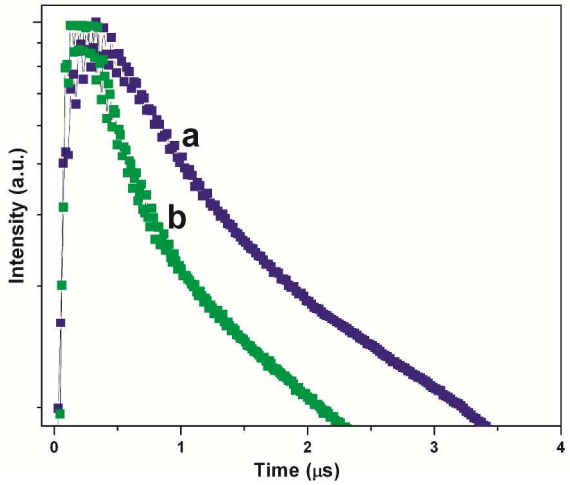

Figure 5. Time resolved photoluminescence spectra (TRPL) show the decay curve of MPS assisted $Sr_{0.975}Ca_{0.975}Eu_{0.05}SiO_4$ phosphor (a) and SiO_2 assisted $SrCaSiO_4:Eu^{2+}$ phosphor (b) for λ_{ex} = 266 nm and λ_{em} = 595 nm.

To confirm the simulation results, a prototype white LED lamp model had been fabricated by embedding a 400 nm ultra-violet and 450 nm blue LED chips with various concentrations of MPS assisted $Sr_{0.975}Ca_{0.975}Eu_{0.05}SiO_4$ phosphor. Figure 4B shows the emission behaviour and digital image of warm-white LED lamp which results with CCT of 3350 & 3100 K under 400 nm & 450 nm LEDs, respectively. The CRI under same excitations are found to be 81 & 80, respectively. The corresponding color point of this LED lamp is indicated by green dots (P1 & P2) in the CIE diagram (Figure 4A). Earlier reports, confirmed the production of warm white light with the phosphor whose CCT < 4000 K and CRI > 80. This confirms that the MPS assisted $Sr_{0.975}Ca_{0.975}Eu_{0.05}SiO_4$ phosphor is quite efficient to make a warm white light under UV and blue LED chips. It was also compared with prototype LEDs fabricated with commercial YAG:Ce which showed an emission at 550 nm under an excitation of 450 nm. Moreover, the lack of energy absorption at 400 nm results in the absence of emission under 400 nm LED chip (Figure S4). Finally, the time resolved photoluminescence (TRPL) properties were measured to understand the decay time of Eu^{2+} emission and presented in Figure 5. The decay curve of MPS assisted $Sr_{0.975}Ca_{0.975}Eu_{0.05}SiO_4$ and SiO_2 assisted $SrCaSiO_4:Eu^{2+}$ phosphors are fitted well with double- exponential function and confirmed the overlapping of shorter and longer wavelength emission that are originated from two different Eu^{2+} sites as mentioned earlier. The result obtained for MPS assisted $Sr_{0.975}Ca_{0.975}Eu_{0.05}SiO_4$ showed an emission decay time of 0.9 & 1.1 μs at room temperature. This value of decay time is relatively greater than that recorded for $SrCaSiO_4:Eu^{2+}$ synthesized in the absence of MPS (0.6 & 0.7 μs). This may be due to the non-radiational energy transfer between the energy levels which in-turn lead to the emission at higher wavelength (low energy) for MPS assisted $Sr_{0.975}Ca_{0.975}Eu_{0.05}SiO_4$ phosphor. This value is in accord to the literature reported decay time of $Eu^{2+}4f^65d^1 \rightarrow 4f^7$ emission in solids.[16]

So, it is noteworthy that the MPS assisted $Sr_{0.975}Ca_{0.975}Eu_{0.05}SiO_4$ shows a broad emission from blue to red along with all the properties needed for warm-white LEDs while the other conventional Eu^{2+} doped phosphors show blue, green emissions. There are only a few reports on the orange and red emitting Eu^{2+} based phosphor synthesized using water soluble silica[11] through sol-gel technique and SiO_2 through solid-state method.[8] But, our material is synthesized by adopting a facile wet-solid phase reaction method in the presence of a unique and diversified material of application, called mesoporous silica as silicate source. This synthesis strategy is the first of its kind and thus acclaiming its novelty.

Conclusions

In summary, a yellow emitting MPS assisted $Sr_{0.975}Ca_{0.975}Eu_{0.05}SiO_4$ phosphor had been synthesized using mesoporous silica as silicate source for the first time through a simple wet-solid phase reaction method. The MPS assisted $Sr_{0.975}Ca_{0.975}Eu_{0.05}SiO_4$ phosphor exhibits a broad yellow emission starting from blue to red region along with the required red components in it. It also showed good thermal stability and good color emitting stability against temperature till 450 K. Warm white light along with the CCT < 4000 K and CIE > 80 had been achieved when the MPS assisted $Sr_{0.975}Ca_{0.975}Eu_{0.05}SiO_4$ phosphor blended with UV and blue LEDs. The present work demonstrates the production of warm-white light with high color rendition by a single-dopant activated host, which is not reported

before. Moreover, the utilization of mesoporous silica for synthesizing silicate phosphors is described here for the first time. These considerations will simply drive the train of thoughts in making a viable platform for the utilization of different kinds of porous silica as silicate sources towards the synthesis of efficient phosphors of unprecedented efficacy.

Experimental Section

Materials synthesis

Preparation of Mesoporous silica (MPS)

Mesoporous silica was synthesized by following our previous report[13]where Pluronic (P-123) was used as structure directing agent. In a typical synthesis, 3.6 g of P-123 was dissolved in 140 g of 2N HCl in which 3.6 g of glycerol was added. It was stirred for 4h at room temperature, and 4 g of TEOS was added as silica source. After 5 min of vigorous stirring, the reaction mixture was kept under static condition for overnight and then it was transferred to a Teflon flask and kept for aging at 100 °C for 24 h. The white precipitate obtained was then filtered, washed and dried under vacuum at 80 °C. It was then calcined at 550 °C for 6 h in a muffle furnace to remove the organic moieties.

Preparation of MPS assisted$Sr_{0.975}Ca_{0.975}Eu_{0.05}SiO_4$

The phosphor was synthesized through a wet-solid phase reaction method. In a typical synthesis, 0.6 g of MPS was completely dispersed in 10 mL of ethanol by sonication process. The synthesis of MPS can be found in the supplementary information. The cationic sources ($CaCO_3$& $SrCO_3$) were also dispersed in 20 mL of ethanol and mixed along with the MPS dispersion. This mixture was stirred for 30 min and the dopant ($EuCl_3.6H_2O$) was added to the same solution. It was then stirred for overnight at 35 °C so as to allow the cationic and dopant ions to get adsorbed into the mesoporous channels. Then the temperature is increased slowly to 60 °C. It was stirred till the ethanol gets vaporized and ground well using a mortar and pestle. The powdered sample was calcined at 600 °C for 5 h to remove the organic moieties from the sample and treated at 1200 °C under reduced atmosphere (95 % N_2& 5 % H_2) for 2 h. The chemical ratio used for the synthesis is 0.975:0.975:0.05:1 (Sr:Ca:Eu:MPS). The synthesized samples are characterized systematically and the detailed informations are given as the supplementary annexure.

Characterization methods

The synthesized $Sr_{0.975}Ca_{0.975}Eu_{0.05}SiO_4$ was initially characterized using powder x-ray diffractometer (XRD, X'Pert Pro, PANalytical), to acquire the information on crystal phase purity. The CuKα (λ=0.154 nm) radiation was used, and the scan was performed from (2θ=) 10° to 80° at the scan speed of 0.01°/sec. The generated XRD data was compared with PCPDFWIN and ICSD for further understanding of the crystal structure of synthesized phosphor.

The internal and external morphologies of MPS and $Sr_{0.975}Ca_{0.975}Eu_{0.05}SiO_4$ phosphor were studied using electron microscopic technique. Field emission scanning electron microscope (FE-SEM, Tescan, MIRA IILMH, Brno, Czech Republic), was operated at a voltage of 15 kV while Field emission transmission electron microscope (FE-TEM, JEM 2100F, JEOL, Japan), was run at 200 kV. Further, the diffraction behaviour and elemental composition were analyzed using selected area electron diffraction (SAED) and energy dispersive x-ray spectroscopic (EDS, model no. 6498, OXFORD, USA) analysis which was in phase with TEM. Nitrogen physisorption isothermal analysis (Autosorb–1, Quantachrome, USA) was performed to analyze the surface and pore properties of MPS after the requisite degassing process at 500 °C for 5h. Brunauer–Emmett–Teller (BET) theory was used to analyze the surface area while Barrett-Joyner-Halenda (BJH) theory was used to calculate the pore size and pore volume.

The luminescence excitation and emission spectra is measured using fluorescence spectrophotometer (FL, RF–5301PC, Shimadzu, Japan) with a Xe lamp as the excitation source. Quantum efficiency (QE) of $Sr_{0.975}Ca_{0.975}Eu_{0.05}SiO_4$ phosphor was measured using a spectrofluorimeter equipped with an integrating sphere (ISF-513). For the temperature dependent emission intensity measurements, the sample was mounted on a homemade heating unit consisting of a copper sample holder, a cartridge heater and a temperature controller. A conventional ultra violet lamp of 385 nm wavelength was employed as an excitation source. The temperature was increased gradually from 373 K to 473 K and then decreased without a cooling system starting from 473 K to 373 K and the corresponding emission intensity is recorded at a temperature interval of 10 °C.

The luminescence life time was measured under 266 nm of excitation from a pulsed Nd:YAG laser. The emission wavelength was set as 595 nm which was spectrally separated by a monochromator and the signal was detected using a digital oscilloscope.

Finally, the prototype warm white LEDs were fabricated as follows. Initially, the particular ratios of YAG:Ce and MPS assisted $Sr_{0.975}Ca_{0.975}Eu_{0.05}SiO_4$ phosphors were mixed thoroughly in silicon resin. The prepared phosphor resin was then embedded on 400 nm and 450 nm LED chips. The photoluminescence spectra, CRI and CCT of warm white light produced from the prototype LEDs were recorded from the USB 4000 miniature fibre optics spectrometer. The measurements were noted at room temperature.

Acknowledgements

This research was financially supported by Changwon National University (2013–2015).

Notes and references

[a] *Department of Physics, Changwon National University, Changwon, Republic of Korea*
[b] *Centre for Nanotechnology & Advanced Biomaterials, SASTRA University, Thanjavur, India*
[c] *Advanced Materials Division, Korea Research Institute of Chemical Technology, Daejeon, Korea*
[d] *Department of Electronic Material Engineering, Silla University, Busan, Korea*
[e] *Department of Physics, Pukyong National University, Busan, Korea*
[f] *Department of Chemistry, Changwon National University, Changwon, Republic of Korea*
Corresponding Authors: kwjang@changwon.ac.kr; Ph. No. +82-055-213-3427; Fax: +82-55-213-0263

† Electronic Supplementary Information (ESI) available: [BET, SEM, TEM & all other characterizations are given in the ESI]. See DOI: 10.1039/b000000x/

1 F. Schubert and J. K. Kim, *Science,* 2005, **308**, 1274; J. M. Phillips, M. E. Coltrin, M. H. Crawford, A. J. Fischer, M. R. Krames, R.Mueller-Mach, G. O. Mueller, Y. Ohno, L. E. S. Rohwer, J. A. Simmons and J. Y.Tsao, *Laser & Photon. Rev.,* 2007, **1**, 307; A. Zukauskas, M. S. Shur and R. Caska, Introduction to Solid-State Lighting. John Wiley and Sons, Inc.: New York, 2002; S. Nakamura and G. Fasol, The blue laser diode, Springer-Verlag: Berlin, 1997.

2 M. Yamada, Y. Narukawa, H. Tamaki, Y. Murazaki and T. Mukai, *IEICE Trans. Electron.,* 2005, **E88C**, 1860; M. S. Shur and A. Zukauskas, *Proc. IEEE,* 2005, **93**, 1691; S. Pimputkar, J. S. Speck, S. P. DenBaars and S. Nakamura, *Nature Photon.,* 2009, **3**, 180.

3 M. R. Krames, O. B. Shchekin, R. Mueller-Mach, G. O. Mueller, L. Zhou, G. Harbers and M. G. Craford, *J. Disp. Techn.,* 2007, **3**, 160.

4 T. Taguchi, *IEEJ Trans.,* 2008, **3**, 21.

5 S. Ye, F. Xiao, Y. X. Pan, Y. Y. Ma and Q. Y. Zhang, *Mater. Sci. Eng. R-Rep.,* 2010, **71**, 1.

6 A. Setlur, *Electrochem. Soc. Interface,* 2009, **18**, 32; W. D. Wang, J. K. Tang, T. H. Sheng, J. Wang and B. P. Sullivan, *Chem. Phys. Lett.,* 2008, **457**, 103; X. Yi, S. Zhou, C. Chen, H. Lin, Y. Feng, K. Wang and Y. Ni, *Ceram. Int.,* 2014, **40**, 7043.

7 N. Kimura, K. Sakuma, S. Hirafune, K. Asano, N. Hirosaki and R. J. Xie, *Appl. Phys. Lett.,* 2007, **90**, 051109; A. Aboulaich, M. Michalska, R. Schneider, A. Potdevin, J. Deschamps, R. Deloncle, G. Chadeyron and R. Mahiou, *ACS Appl. Mater. Interfaces,* 2014, **6**, 252; A. Setlur, W. J. Heward, M. E. Hannah and U. Happek, *Chem. Mater.,* 2008, **20**, 6277.

8 T. L. Barry, *J. Electrochem. Soc.,* 1968, **115**, 1181; J. Brgoch, C. K. H. Borg, K. A. Denault, A. Mikhailovsky, S. P. DenBaars and R. Seshadri, *Inorg. Chem.,* 2013, **52**, 8010; M. PardhaSaradhi and U. V. Varadaraju, *Chem. Mater.,* 2006, **18**, 5267; S. H. M.Poort, H. M. Reijnhoudt, H. O. T. Van der Kuip and G.Blasse, *J. Alloy. Compd.,* 1996, **241**, 75.

9 S. H. M. Poort, W. P. Blockpoel and G. Blasse, *Chem. Mater.,* 1995, **7**, 1547. W; Zhi-Jun, Y. Z. Ping, G. Q. Lin, L. P. Lai and F. G.Sheng, *Chinese Phys. B,* 2009, **18**, 2068; S. H. M. Poort and G. Blasse, *J. Lumin.,* 1997, **72-74**, 247.

10 M. Catti, G. Gazzoni and G. Ivaldi, *ActaCryst.,* 1984, **B40**, 537.

11 S. Tezuka, Y. Sato, T. Komukai, Y. Takatsuka, H. Kato and M. Kakihana, *Appl. Phys. Express,* 2013, **6**, 072101.

12 S. Gandhi, K. Thandavan, B. J. Kwon, H. J. Woo, K. Jang and D. S.Shin, *Ceram. Int.,* 2014, **40**, 5245.

13 T. Kresge, M. E. Leoniwics, W. J. Roth, J. C. Vartuli and J. S. Beck, *Nature,* 1992, **359**, 710; S. Gandhi, S. Sethuraman and U. M. Krishnan, *J. Porous Mater.,* 2011, **18**, 329; S. Gandhi, K. Thandavan, B. J. Kwon, H. J. Woo, S. S. Yi, H. S. Lee, J. H. Jeong, K. Jang and D. S. Shin, *RSC Adv.,* 2014, **4**, 5953; S. Gandhi, S. Venkatesh, U. Sharma, N. R.Jagannathan, S.Sethuraman and U. M.Krishnan, *J. Mater. Chem.,* 2011, **21**, 15698.

14 R. D. Shannon, *ActaCryst.,* 1976, **A32**, 751.

15 W. J. Park, Y. H. Song and D. H. Yoon, *Mater. Sci. Eng. B-Adv.,* 2010, **173**, 76; H. Yu, Y. Lai, G. Gao, L. Kong, G. Li, S. Gan and G. Hong, *J. Alloy. Compd.,* 2011, **509**, 6635.

16 S. H. M. Poort, A. Meyerink and G. Blasse, *J. Phys. Chem. Solids,*1997, **58**, 1451; X. Li, J. D. Budai, J. Y. Howe, J. Zhang, X. J. Wang, Z. Gu, C. Sun, R. S. Meltzer and Z. Pan, *Light Sci. Appl.,* 2013, DOI: 10.1038/lsa.2013.6.

Graphical Abstract

Highly efficient warm white light emitting Eu^{2+} activated silicate host: Another fabulous work of mesoporous silica

Sakthivel Gandhi,[a,b] Kavitha Thandavan,[b] Bong-Joon Kwon,[a] Hyun-Joo Woo,[a] Chang Hae Kim,[c] Soung Soo Yi,[d] Jung Hyun Jeong,[e] Dong-Soo Shin[f] and Kiwan Jang*[a]

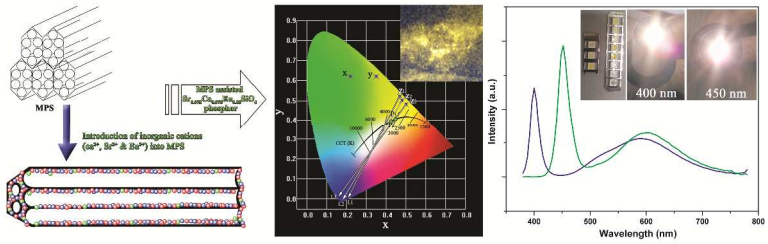

The inception of a new silicate source namely MPS (mesoporous silica) for the synthesis of $Sr_{0.975}Ca_{0.975}Eu_{0.05}SiO_4$ phosphor shows an excellent emissive property along with the suffice red spectral components. It is a promising feature for replacement of the existing conventional YAG:Ce, to obtain warm white light using LEDs.